Journal of Achievements in Materials and Manufacturing Engineering

VOLUME 39
ISSUE 2
April
2010

AgSnBi powder consolidated by composite mode of deformation

M. Richert [a,*], J. Richert [a], B. Leszczyńska - Madej [a], A. Hotloś [a], M. Maślanka [b], W. Pachla [c], J. Skiba [c]

[a] Faculty of Non-Ferrous Metals, AGH University of Science and Technology, Al. Mickiewicza 30, 30-059 Kraków, Poland

[b] Faculty of Mechanical Engineering & Robotics, AGH University of Science and Technology, Al. Mickiewicza 30, 30-059 Kraków, Poland

[c] Institute of High Pressure Physics Unipress, Warszawa, Poland

* Corresponding author: E-mail address: mrichert@agh.edu.pl

Received 03.02.2010; published in revised form 01.04.2010

Materials

ABSTRACT

Purpose: The objective of this work present the characterization of microstructure and properties of consolidated powder AgSn7.5Bi0.5 by using composition of cyclic extrusion compression (CEC) and hydrostatic extrusion (HE) methods. As the final product the wires of 3 mm in diameter were obtained. The comparison of powder properties after CEC deformation and after the combined deformation CEC and HE is presented.

Design/methodology/approach: The investigated samples contained consolidated by large plastic deformations particles of AgSnBi. The samples were deformed by the CEC method in the range of true strains = 0.32 up to φ= 25.2 and then additionally were extruded to φ = 1.85. The systematic observations by optical microscopy were performed for determination of the quality of particle joints. The microstructure was observed by optical, scanning and transmission electron microscopy. Microhardness was measured and areas around indentations of microhardness penetrator were observed. This allows evaluated resistance of consolidated material against local cracking under the penetrator load.

Findings: Microstructure of consolidated AgSnBi powder was finding at the cross sections of samples as consisting from almost equiaxial grains, which size decreasing with the increasing of plastic deformations. The microhardness of samples strongly increase in the few first cycles (to about φ = 2 of CEC) and then keeps almost the same level of about μHV = 107 - 111 to the strain of about φ= 25. Inside the consolidated granules subgrains/grains with the average size of about 77 nm, after the φ = 25, were found.

Research limitations/implications: This paper presents results for one alloy - MC MgAl3Zn1 only, cooled with three different solidifications rate i.e. 0.6, 1.2 and 2.4°C/s, for assessment for the liquidus and solidus temperatures and its influence on the mechanical properties and structure.

Practical implications: The parameters described can be applied in metal casting industry for selecting magnesium ingot preheating temperature for semi solid processing to achieve requirements properties.

Originality/value: The paper contributes to better understanding and recognition an influence of different solidification condition on non-equilibrium thermal parameters of magnesium alloys.

Keywords: Thermal treatment; Magnesium alloys; Mechanical properties

Reference to this paper should be given in the following way:

M. Richert, J. Richert, B. Leszczyńska-Madej, A. Hotloś, M. Maślanka, W. Pachla, J. Skiba, AgSnBi powder consolidated by composite mode of deformation, Journal of Achievements in Materials and Manufacturing Engineering 39/2 (2010) 161-167.

© Copyright by International OCSCO World Press. All rights reserved. 2010

1. Introduction

Owing to their high electrical and thermal conductivities, high resistance to arcing, high welding adhesion resistance, low contact resistance, high hardness and strength, silver metal oxides (Ag/MeO), especially silver cadmium oxide (Ag/CdO), have found wide application in electrical and electronics industries. Being pollution-free, silver tin oxide (Ag/SnO_2) has been used to replace toxic Ag/CdO contact materials in last two decades [1,2].

In order to compensate the shortcoming of Ag/SnO_2 materials, Ag/ZnO contact material has been developed. Electrical contact resistance of Ag/ZnO is lower and is a potential candidate to replace Ag/CdO as new contact material.

In terms of replacing cancerous Ag-CdO also an attempt has been made to synthesize Ag-Fe binary system for electrical contacts [3]. This could be made via conventional foundry route using specially developed mixing method of rotation-cylinder method (RCM) and through subsequent extrusion, drawing and riveting procedures.

The system Ag-Sn is a key system for lead free solder materials, and has been extensively studied in the past for various other reasons [4]. The small additions of Bi and/or Zn are frequently used to adjust an appropriate melting regime of lead free solder alloys for different applications. In details the Ag-Bi-Sn system was carried out in the work [5]. A study of silver-based contact materials free of Cd was presented in the work [6,7,8,9].

Nowadays a great focus is directed to silver alloys. The stabilization of mechanical properties of silver alloys is presented in paper [10]. The author found that rare earth metals contributed to fine structure obtaining. The new composite materials can be formed on the base of silver, as it is reported in the work [11,12]. The silver composites were produced by addition of SiC and Al_2O_3 particles. It is reported that manufacturing of this type of composites is based most of all on the utilization of powder metallurgy techniques. Silver is also used for nanoparticle manufacturing [13].

A large usefulness of silver and silver alloys contribute to more and more scientific interest of methods of their production and structure and properties improvement.

There are several successful methods including powder metallurgy (PM) and internal oxidation (IO) to prepare contact materials [14]. However still the investigation on other mechanisms of consolidation of powder precursors for production bulk electric contact materials are carry out.

The flow of cohesive powder is a difficult phenomenon to understand due to the complex behavior of the interacting particles in the material. The powders are consolidated into products with a given shape. The basic steps in powder metallurgy are therefore powder production and powder consolidation [15]. The consolidation is achieved by various techniques such as pressing, hot extrusion, hot isostatic pressing forging and others. The effect of high compressive pressure on the final densification of consolidated powders is high level of hardness and essential lowering of porous [6,16,17].

The present work is to study the combined effects of the Cyclic Extrusion Compression and hydrostatic extrusion on the consolidation of AgSnBi powder. The final product can attain properties useful for electric contact material.

2. Experimental basis

The powder AgSnBi of 40 μm of mean size was mechanically consolidated by using Cyclic Extrusion Compression (CEC) method [8] in the range of deformations $\varphi = 0.42 - 25.3$ (corresponds to 1 - 60 CEC cycles of deformation). The $\varphi = 0.42$ deformation was exerted in a single CEC cycle. After the CEC consolidation samples were extruded by hydrostatic extrusion method developed in Institute of High Pressure Physics Unipress in Warsaw to deformation $\varphi = 1.85$. The wires of 3 mm in diameter were obtained as a final product of the combined deformation. Additionally the samples prepared by the as-sintering technique was investigated.

The microstructure of samples consolidated by the CEC method and also after the complex deformation consisting from CEC deformation and hydro extrusion, was characterized by optical microscopy (Olympus GX51) and scanning electron microscopy Tesla BS301. Thin foils were observed by JEOL 2010 ARB transmission electron microscopy.

The samples to optical microscopy observations were polished mechanically applied Struers equipment and technique. They were grinded, then polished in diamond pastes and finally in the suspension OPS. Thin foils, for TEM investigations, were prepared from cross sections by cutting, grinding and ion sputtering, using Struers and Gatan instruments.

Dispersion parameters such as subgrain, grain and particle powder radius were measured and evaluated by means chord parameter.

The measurement of microhardness was carried out on polished samples at room temperature using a Vickers hardness tester PMT3 at load 100 G.

3. Investigation results and discussion

After the CEC deformation the AgSnBi powder has been consolidated into the bulk material just after the few first CEC cycles. The examples of the microstructure observed after 3 CEC cycles ($\varphi = 1.3$) is presented in Fig. 1.

In comparison Fig. 2 presented optical image after the 60 CEC cycles ($\varphi = 25.3$). The finding microstructure refinement, has been confirmed by the mean chord parameter measurement (Fig. 3). It was found that particle size diminished of about two times after the 60 CEC cycles. The initial powder particles had size of about 40 μm, and after the $\varphi = 25.3$ (60 CEC cycles) mean size of AgSnBi particles exhibit value of about 18 μm.

Characteristic feature of consolidated samples is their complex internal microstructure, which consists from numerous very small particles. Especially it is visible after the $\varphi = 25.3$ (60 CEC cycles). At lower values of deformation the large particles, consisting from agglomerated small particles, were bonded by darker areas, which probably contained micro-voids and some oxides. After the $\varphi = 25.3$ (60 CEC cycles) the bonds disappeared and only the uniform microstructure was observed.

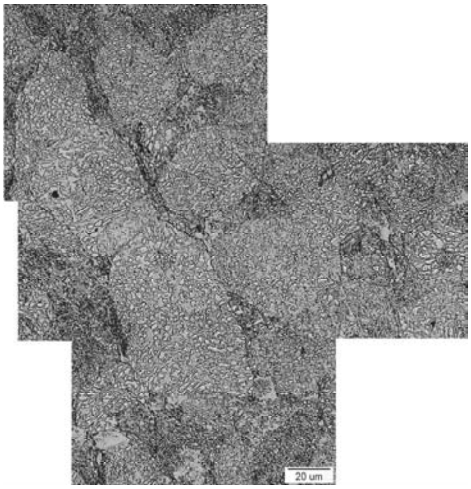

Fig. 1. Optical microscopy image, microstructure of AgSnBi after φ = 1.3 (3 CEC cycles)

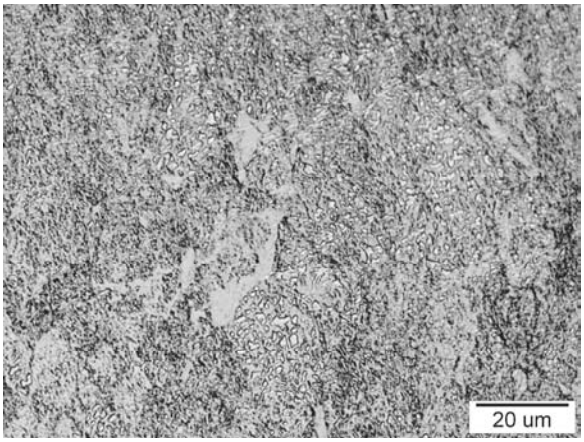

Fig. 2. Optical microscopy image, microstructure of AgSnBi after φ = 25.3 (60 CEC cycles)

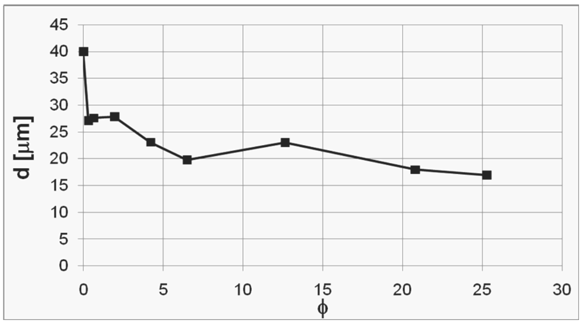

Fig. 3. Mean chord of AgSnBi particles after the CEC proces of consolidation versus deformation exerted in CEC

The example of the wire microstructure obtained by the combination of cyclic extrusion compression and hydrostatic extrusion, observed by optical microscopy is presented in Fig. 4. After 0.5 CEC cycle (φ = 0.21) lamellar microstructure developed with characteristic shear bands penetrating cross section of samples with the inclination of about 50^{o} to the extrusion direction. Shear bands are very characteristic feature of severe deformed microstructures and indicated on the intense hardening of the material.

Microstructural details of the consolidated powder are shown in scanning electron micrographs in Fig. 5. The scanning electron micrographs characterized general aspect of the mechanically consolidated samples. Numerous shear bands appeared in microstructure.

Shear bands form distinct deflections of the material bands flowing accordingly extrusion direction. Very characteristic is existence of two mutually crossing sites of shear bands. After 0.5 CEC cycle (φ = 0.21) some oxides existing on powder particle surfaces and not completely destroyed during the CEC process of deformation is probably responsible for black lines into microstructure between the observed bands.

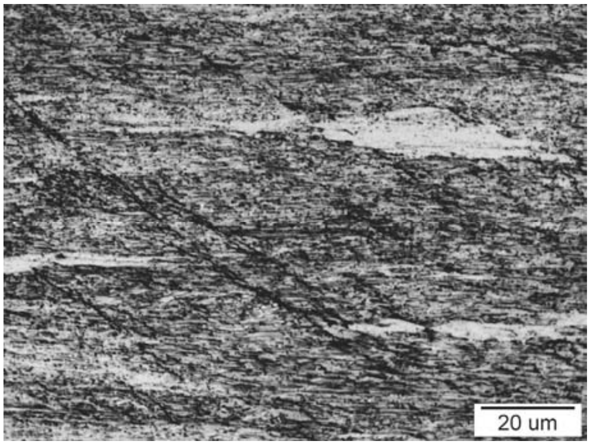

Fig. 4. Optical microscopy image, microstructure after combined deformation, CEC (φ = 0.21, 0.5 cycle) and hydrostatic extrusion (φ = 1.8)

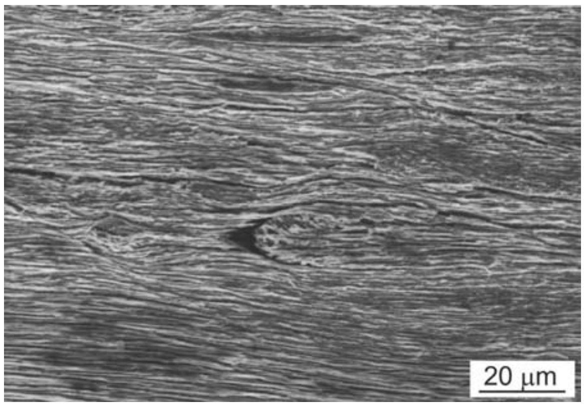

Fig. 5. Scanning microscopy image corresponding to φ = 0.21, by 0.5 of CEC cycles and hydrostatic extrusion (φ = 1.8)

The micrographs corresponding to 3 CEC cycles (φ = 1.26) and additional hydrostatic extrusion to φ = 1.8 are presented at Fig. 6 (optical microscopy image) and Fig. 7, Fig. 8 (scanning microscopy images). In Fig. 6 different regions exist, containing bands with very various thickness. The similar features of microstructure can be also distinguished in Fig. 7 and Fig. 8. Especially in Fig. 8 the distinct deflections of bands suggest large shear deformation in samples.

It was found that the previous deformation by CEC strongly influence on the final wire microstructure. With the increase of the CEC deformation the diminishing of shear bands width and increase of their density was observed. If after the 0.5 CEC cycle and hydrostatic extrusion the mean distance between the shear bands is about 20 μm, after 3 CEC cycles and successive hydrostatic extrusion this distance decreasing to about 10 μm. It suggests that simultaneously the density of shear bands should be essentially increases in the whole volumes of samples.

Shear bands becomes clearly distinguishable especially at higher magnifications as it is visible in Fig. 8, and in Fig. 9.

The reported changes of the distance between the shear bands it is possible find by the comparison of microstructures showing in Fig. 4 - Fig. 9.

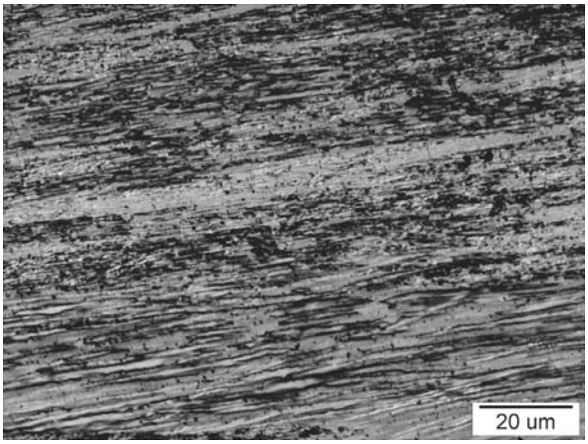

Fig. 6. Optical microscopy image, microstructure after 3 CEC cycles (φ = 1.26, 3 cycle) and hydrostatic extrusion (φ = 1.8)

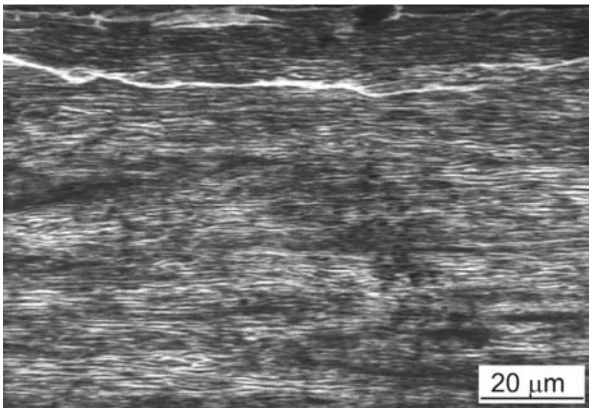

Fig. 7. Scanning microscopy image corresponding to deformation φ = 1.26, by 3 CEC cycles and hydrostatic extrusion (φ = 1.8)

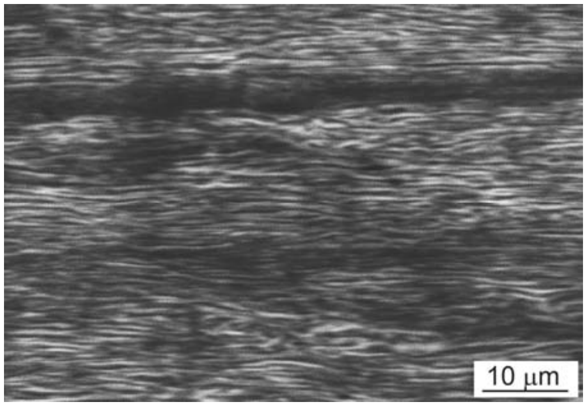

Fig. 8. Scanning microscopy image corresponding to deformation φ = 1.26 , by 3 CEC cycles and hydrostatic extrusion (φ = 1.8)

The existence of shear bands in the consolidated microstructures indirectly indicates that the rate of densification of AgSnBi is good and uniform. About this proofs the continuity of plastic deformation in shear bands thorough the sample section.

The increase of the combined deformation, corresponding generally to the increase of the CEC cycles, is the reason of continuous diminishing of microstructure elements, both the diminishing of the shear bands distance and also thickness of lamellar bands of alloy flowing accordingly extrusion direction. The process of the microstructure diminishing at the beginning of deformation was very intensive, however as the deformation increases its intensity becomes slower.

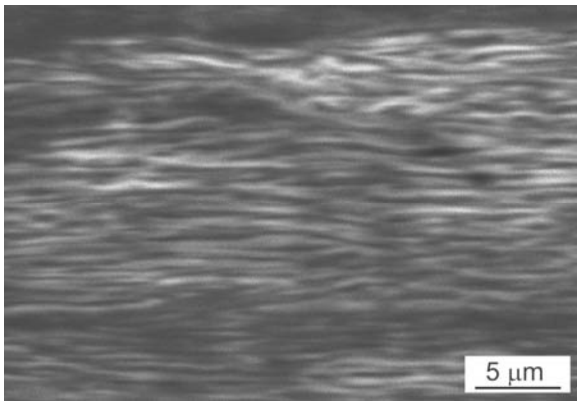

Fig. 9. Scanning microscopy image corresponding to deformation φ = 1.26 , by 3 CEC cycles and hydrostatic extrusion (φ = 1.8)

Fig. 10 and Fig. 11 exhibit typical examples of scanning microscopy images of consolidated AgSnBi powder with the characteristic microstructure with shear bands and lamellar flow bands. After the 20 CEC cycles the lamellar flow bands are divided by shear bands into shorter sections, which could be clearly observed in Fig. 12.

The process of lamellar, material bands division by crossing shear bands, after 30 CEC cycles and additional hydrostatic extrusion leads to the formation of new microstructure type, consisting from very fine granules with the dimension of about a few μm (Fig. 12). On this background the new family of long macroscopic shear bands develops crossing again the new formed microstructure.

Probably by such a way the intense rotation and densification of powder is provided, which assure obtained good consolidation of powder granules. About the quality of consolidation proofs detailed observations of microhardness tester penetrator indentations and effects of material deformation around the indentations. No cracks and voids in material around microhardness indentations were found (Fig. 13).

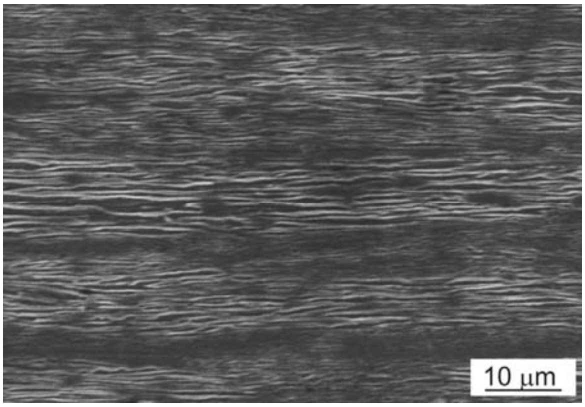

Fig. 10. Scanning microscopy image corresponding to deformation $\varphi = 4.2$, by 10 CEC cycles and hydrostatic extrusion ($\varphi = 1.8$)

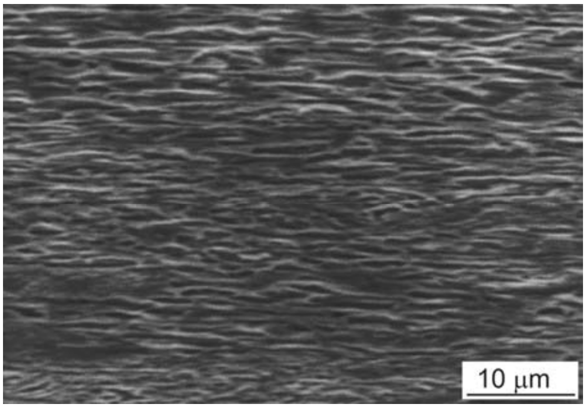

Fig. 11. Scanning microscopy image corresponding to deformation $\varphi = 8.4$, by 20 CEC cycles and hydrostatic extrusion ($\varphi = 1.8$)

In comparison, to mechanically consolidated AgSnBi samples by intense deformation, the microstructure after the as-sintering process is presented in Fig. 14. The very fine grains were found and some roughness of the outer surface.

The TEM microstructure of as-sintered samples is shown in Fig. 15. The large subgrains with the particles placed in the subboundaries were observed in the microstructure. Besides the large particles also very small ones inside the subgrains were found. This suggest that the solid solution is depleted from the chemical element components by the mechanism of particle precipitation. The effect of this phenomenon is lowering of hardening level of the alloy.

Contrary to this image the mechanically consolidated samples after the CEC exhibit very small subrains/grains with the average diameter of about 100 nm with the numerous nano-twins inside (Fig. 16). There were no found large particles or precipitations in the mechanically consolidated samples. The subgrain boundaries were find free from particles.

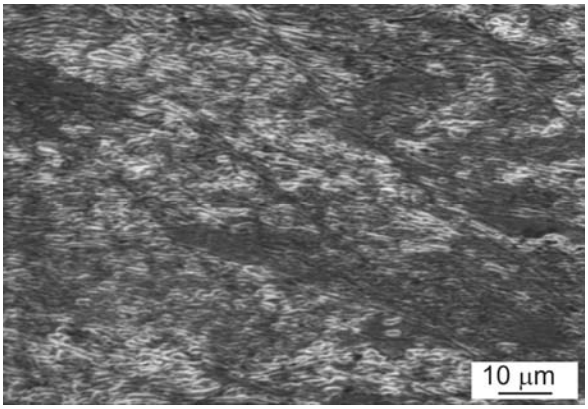

Fig. 12. Scanning microscopy image corresponding to deformation $\varphi = 12.6$, by 30 CEC cycles and hydrostatic extrusion ($\varphi = 1.8$)

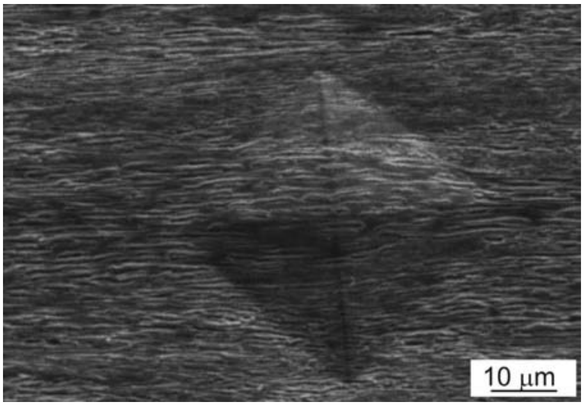

Fig. 13. Scanning microscopy image corresponding to deformation $\varphi = 8.4$, by 20 CEC cycles and hydrostatic extrusion ($\varphi = 1.8$)

It is fairly well established that a finer microstructure element size results in a higher hardness for the consolidated bulk samples of materials. Fig. 17 presented the comparison of the microhardness of samples consolidated only by CEC, the mirohardness of samples deformed by combination of CEC and hydrostatic extrusion and additionally the level of microhardness of AgSnBi after as-sintering process is shown. The plot after the combined mode of deformation exhibit the highest level of microhardness. A notable difference between the CEC consolidation process and combined consolidation process could be notice. The increase of about 20 % of microhardness in samples consolidated by combined deformation was found. The lowest level of microhardness exhibit sample after the sintering. The microhardness of the as-sintered AgSnBi powder is lower of about 40% in comparison to microhardness of samples consolidated by combination of CEC and hydrostatic extrusion.

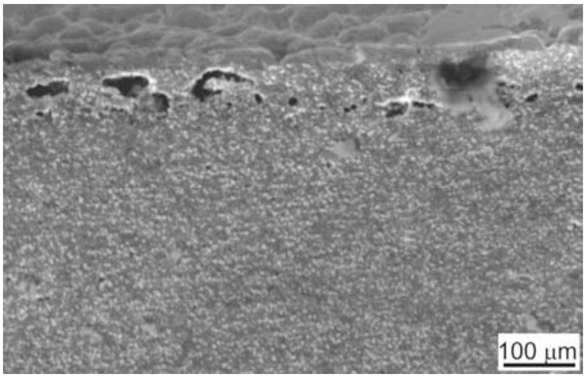

Fig. 14. Scanning microscopy image of as - sintered AgSnBi sample, magnification 300x

Fig. 15. TEM microscopy image of as - sintered AgSnBi sample

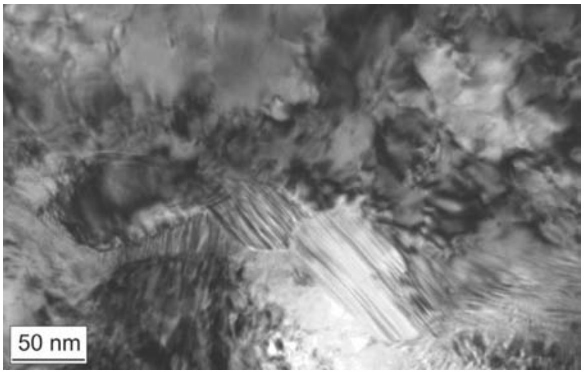

Fig. 16. TEM microscopy image of consolidated by CEC (φ = 13.44, 32 CEC cycles)

The results suggest that samples consolidated by plastic deformation in the CEC process or by combination of CEC and further hydrostatic extrusion exhibit much higher rate of densification than the only as-sintered samples. Under both mode of deformation samples attained good consolidation, which could be evaluated indirectly by the level of microhardness. Mechanically consolidated samples show quite good properties of the AgSnBi material.

The microstructures observed at the perpendicular sections of samples after the CEC and hydrostatic extrusion consist from the almost equiaxial granules joined by fraction of dark material probably contained oxides forming on the particle surfaces, AgSnBi material taking part in the surface processes of mechanical cohesion of powder particles and some micro-voids.

The typical example of this type of microstructure, observed by optical microscopy, is presented in Fig. 18, corresponding to φ = 4.2, 10 CEC cycles and φ = 1.85 by HE.

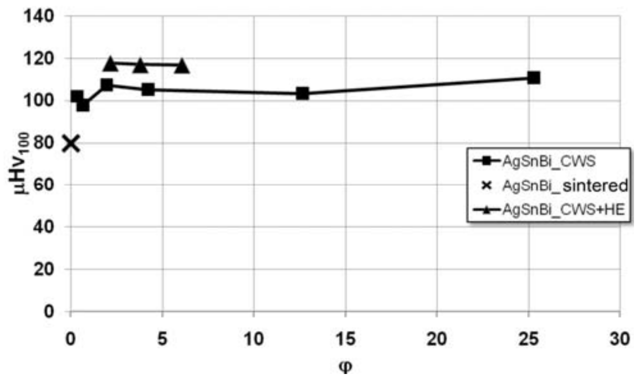

Fig. 17. Microhardness of samples consolidated by CEC, by combined mode of deformation - CEC and hydrostatic extrusion and for comparison, the microhardness of the AgSnBi obtained by sintering

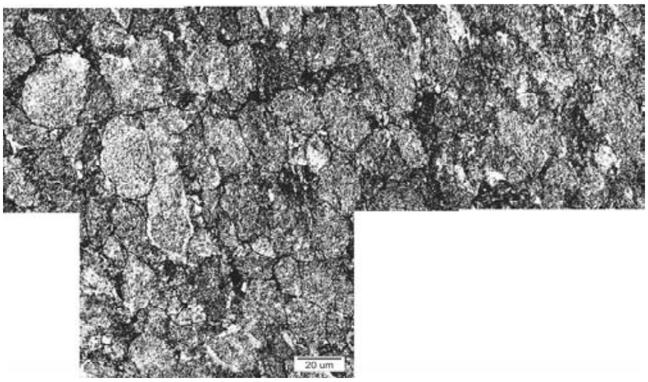

Fig. 18. Optical micrograph of AgSnBi microstructure observed after φ = 4.2, 10 CEC cycles and φ = 1.85 by HE

Inside the particles is possible to distinguish fine grains/molecules which coalescence during deformation simultaneously with the removing of pores and micro-voids. It causes formation of large equiaxial granules.

4. Conclusions

The following conclusion may be drown from the performed investigations:

- The AgSnBi powder, consolidated by the complex mode of deformation, consisting from Cyclic Extrusion Compression and Hydrostatic Extrusion, exhibit microhardness of about 20% higher than powder consolidated only by CEC.
- In the all investigated wire samples after complex deformation mode, the shear bands were observed, which density depends strongly on the level of the exerted strains.
- Inside the consolidated particles the subgrains (nanograins) were found with the mean size of about 100 nm with the numerous twins inside.

Acknowledgements

The authors would like to acknowledge the financial support provided by project No PBZ-MNiSW-3/3/2006.

References

[1] C.P. Wu, D.Q. Yi, J. Li, L.R. Xiao ,B. Wang, F. Zheng , B. Wielage, A. Wank, Investigation on microstructure and performance of Ag/ZnO contact material, Journal of Alloys and Compounds 457 (2008) 565-570.

[2] C.P. Wu, D.Q. Yi, C.H. Xu, J. Li, B. Wang, F. Zheng, Microstructure of internally oxidized layer in Ag-Sn-Cu Allom, Corrosion Science 50 (2008) 3508-3518.

[3] K. Kim Shae, Novel rotation-cylinder method for the processing of binary alloys with no range of solid solubility, Materials Science and Engineering A 449-451 (2007) 752-755.

[4] H. Ipser, H. Flandorfer, Ch. Luef, C. Schmetterer, U. Saeed, Thermodynamics and phase diagrams of lead-free solder, Materials, Journal of Materials Science Mater Electron 18 (2007) 3-17.

[5] S. Hassam, E. Dichi, B. Legendre, Experimental equilibrium phase diagram of the Ag-Bi-Sn system, Journal of Alloys and Compounds 268 (1998) 199-206.

[6] S. Księżarek, B. Besztak, Wires used in the production of electric contacts, Wire Journal International 40 (2000) 208-213.

[7] L.P. Lechman, R.K. Kinyanjui, J. Wang, Y. Xing, L. Zawalij, P. Borgesen, E.J. Cotts, Microstructure and Damage Evolution in Sn-Ag-Cu Joints, Proceedings of the Electronic Components and Technology Conference, 2005, 674-681.

[8] S.K. Kang, Lead, (Pb) - Free Solders for Electronic Packaging, Journal of Electronic Materials 23/8 (1994) 701-707.

[9] I.E. Anderson, F.G. Yost, J.F. Smith, Ch.M. Miller, R.L. Terpstra, Pb-Free Sn-Ag-Cu Ternary Eutectic Solders, United States Patent, 5,527,628, 1996.

[10] W. Głuchowski, Z. Rdzawski, Stabilization of mechanical properties in silver alloys by addition of lanthanides, Journal of Achievements in Materials and Manufacturing Engineering 30/2 (2008) 129-134.

[11] J. Śleziona, J. Wieczorek, M. Dyzia, Mechanical properties of silver matrix composites reinforced with ceramic particles, Journal of Achievements in Materials and Manufacturing Engineering 17 (2006) 165-168.

[12] J. Wieczorek, J. Śleziona, Silver matrix composites reinforced with galvanically silvered particles, Archives of Materials Science and Engineering 28/8 (2007) 475-478.

[13] M. Staszewski, D. Kopyto, K. Becker, A.Wrona, J. Dworek, M. Kwarciński, The X-ray activated reduction of silver (I) solutions as a metod for nanoparticles manufacturing, Journal of Achievements in Materials and Manufacturing Engineering 28/1 (2008) 23-26.

[14] G. Kosec, I. Anzel, M. Bruncko, L. Kosec, Internal oxidation of Ag - alloys with Te, Se and S, Proceedings of the 13th International Scientific Conference "Achievement in Mechanical and Material Engineering" AMME'2005, Gliwice - Wisła, 2005.

[15] A.K. Eksi, A.H. Yuzbasioglu, Effect of sintering and pressing parameters on the densification of cold isostatically pressed Al and Fe powders, Materials and Design 28/4 (2007) 1364-1368.

[16] F.B. Swinkels, D.S. Wilkinson, E. Arzt, M.F. Ashby, Mechanisms of Hot-Isostatic Pressing, Acta Materialia 31/11 (1993) 1829-1840.

[17] I. Sulima, P. Klimczyk, P. Hyjek, The influence of the sintering conditions on the properties of the stainless steel reinforced with TiB2 ceramics, Archives of Materials Science and Engineering 39/2 (2009) 103-106.